

Formation of Gas-Phase Methyl Radicals over MgO

Daniel J. Driscoll, Wilson Martir, Ji-Xiang Wang, and Jack H. Lunsford*

Contribution from the Department of Chemistry, Texas A&M University, College Station, Texas 77843. Received March 5, 1984

Abstract: When methane was passed over MgO at temperatures of approximately 500 °C, methyl radicals were produced on the surface, released into the gas phase, and trapped downstream in a solid argon matrix where they were analyzed by EPR spectroscopy. Significant differences in initial activity were observed, depending on whether the MgO was pretreated under vacuum or a flow of oxygen. Vacuum conditioning led to essentially no activity while oxygen conditioning resulted in substantial radical production. The oxidant of choice was also critical. Nitrous oxide resulted in a continuous decline of activity while in the presence of oxygen the formation of radicals was at a steady state. Doping of MgO with lithium, sodium, or iron was also examined. Lithium was found to greatly increase the activity up to a doping level of approximately 15.0 wt %. Two pathways are believed to be responsible for the radical formation. Over pure MgO, intrinsic cation vacancies react with molecular oxygen to give an O⁻ center which can abstract a hydrogen atom from methane to produce the methyl radical. For the lithium-doped samples, substitutional Li⁺ ions react with molecular oxygen to form a [Li⁺O⁻] center which is also capable of abstracting a hydrogen atom from methane.

Introduction

The activation of methane for partial oxidation to formaldehyde or methanol is a subject of intense practical interest. Based on work in our laboratory it has been proposed that methyl radicals may be an integral part of a catalytic cycle,¹ therefore hydrogen atom abstraction becomes a critical step in the activation process. A survey was made of metal oxide catalysts that would promote the formation of methyl radicals into the gas phase. The metal oxides that were examined include SiO₂, Al₂O₃, Bi₂O₃, and MgO, of which MgO was by far the most active.²

A regular ionic lattice of MgO might be expected to be inert; however, the crystals contain a large variety of defects including vacancies, ionic impurities, and trapped charge carriers (electrons or holes). Moreover, the high surface area oxide contains sites of low coordination at edges and corners. The remarkable catalytic activity of MgO for butene isomerization³ and H₂-D₂ exchange⁴ has been attributed to oxygen ions at sites of low coordination.

The reactions of C₁ to C₄ alkanes with the oxygen ions O⁻, O₂⁻, and O₃⁻ have been studied in considerable detail,⁵⁻⁷ but these reactions were stoichiometric rather than catalytic. All three species were found to be reactive, and the order of activity was O⁻ >> O₃⁻ >> O₂⁻. In all cases the initial step is believed to be hydrogen atom abstraction by the oxygen ion to form the neutral alkyl radical, but the radicals were not detected either on the surface or in the gas phase. Related EPR studies, however, have demonstrated that O⁻ ions on Mo/SiO₂ catalysts are capable of abstracting hydrogen from CH₄ to form methyl radicals, at temperatures as low as 77 K.^{1,8}

In the present work it was of interest to determine the nature of the active sites that gave rise to the catalytic formation of methyl radicals. The gas-phase radicals were detected by EPR spectroscopy, using a matrix isolation system in tandem with a catalytic reactor.

Experimental Section

The system used to carry out the matrix isolation experiments has been described in considerable detail elsewhere,^{9,10} and only the most important

features and modifications will be given here. The same experimental system was used for all the radical production reactions.

The reactor was constructed of fused quartz (2.5-cm i.d., 35.8-cm length) and had a thermocouple well centered along its axis which allowed measurement of the temperature along the entire reactor length. A perforated quartz plate was positioned 9 cm from the exit end of the reactor to support the catalyst bed. The reactor was resistively heated over a 23.5-cm length and consisted of a 9.0 cm long reaction zone and a 14.5 cm long preheater zone. A temperature profile of the reaction zone showed a maximum variation of ±2 °C. A gas leak was placed between the exit of the reactor and the collection system, creating a pressure gradient. Pressure in the reaction zone was approximately 0.7 torr while in the collection region the pressure was typically 2 × 10⁻³ torr. The reactions were run at 500 °C unless stated otherwise.

The MgO samples were obtained from three different sources: Fisher Certified ACS Grade designated MgO(F), J. T. Baker Ultrahigh purity designated MgO(B), and Aldrich Gold Label (99.999%) designated MgO(A). The MgO normally was used after conversion to the high-surface-area form. The MgO, as received, was added to deionized water, and the resulting slurry was stirred and heated until only a thick paste remained. The paste was air-dried overnight at 140 °C. This Mg(OH)₂ was then reconverted to the high-surface-area oxide during a pretreatment at elevated temperatures. Metal-doped samples were prepared by adding the metal carbonate (Li₂CO₃, Fisher, Certified ACS 99.0%; Na₂CO₃, Mallinckrodt, Analytical Reagent 99.95%) during the water treatment step. The powders obtained were pressed into thin wafers and broken into approximately 3 × 3 mm chips which were distributed in the reactor between four layers of quartz wool. A normal catalyst charge was approximately 0.50 g.

The argon (99.99%), methane (99.97%), oxygen (99.99%), and nitrous oxide (99.0%) were obtained from Matheson Gas. The argon, oxygen, and nitrous oxide were further dried by passage over a molecular sieve trap. The methane was used as received. Flow rates were regulated with Vacua precision metering valves.

The samples were treated, prior to reaction, under flowing oxygen or vacuum at elevated temperatures. In all cases, other than those presented in Table I, the samples were pretreated in the reactor at 450 °C for 2.5 h under a flow of oxygen (300 cm³ min⁻¹). After the oxygen treatment at the high temperature the samples were cooled to 150 °C while still under oxygen flow. The reactor was then connected to the rest of the system, the oxygen flow was terminated, and the reactor was evacuated. The temperature was then raised to 175 °C, and evacuation was continued for 30 min. The reactor was heated to 500 °C over a period of ca. 16 min, the evacuation was discontinued, and the gas feeds were started. Conditioning under vacuum was accomplished by heating Mg(OH)₂ under vacuum to the desired temperatures for the appropriate amount of time. When the process was completed the temperature was raised to 500 °C, the evacuation was discontinued, and the gas flows were started.

The radicals were collected and analyzed in a solid argon matrix which consisted of a sapphire rod cooled to 13.5 K. The collection period for all samples was 25 min. Collection for the initial activity studies was begun after the feed had passed over the sample for 2 min. Initial contact of the feed gases with the sample often led to slight temperature fluctuations, and this 2-min period allowed sufficient time for these variations

(1) Liu, H.-F.; Liu, R.-S.; Liew, K. Y.; Johnson, R. E.; Lunsford, J. H. *J. Am. Chem. Soc.* **1984**, *106*, 4117.

(2) Martir, W. Ph.D. Dissertation, Texas A&M University, College Station, TX, 1981.

(3) Baird, M. J.; Lunsford, J. H. *J. Catal.* **1972**, *26*, 440.

(4) Coluccia, S.; Tench, A. J. *Proc. Int. Congr. Catal.*, **7th**, 1980 **1981**, B, 1554.

(5) Aika, K.; Lunsford, J. H. *J. Phys. Chem.* **1977**, *81*, 1393.

(6) Takita, Y.; Lunsford, J. H. *J. Phys. Chem.* **1979**, *83*, 683.

(7) Iwamoto, M.; Lunsford, J. H. *J. Phys. Chem.* **1980**, *84*, 3079.

(8) Lipatkina, N. I.; Shvets, V. A.; Kazanskii, V. B. *Kinet. Catal.* **1978**, *19*, 979.

(9) Martir, W.; Lunsford, J. H. *J. Am. Chem. Soc.* **1981**, *103*, 3728.

(10) Driscoll, D. J.; Lunsford, J. H. *J. Phys. Chem.* **1983**, *87*, 301.

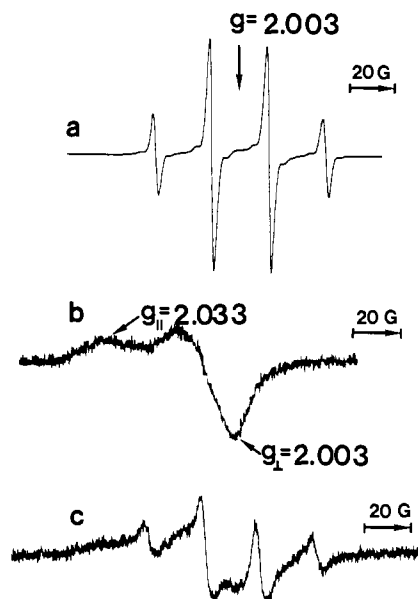


Figure 1. Radical EPR spectra: (a) pure methyl radical ($\text{CH}_3\cdot$) spectrum; (b) pure methyl peroxy radical ($\text{CH}_3\text{O}_2\cdot$) spectrum; (c) mixture of methyl and methyl peroxy radicals spectrum.

to stabilize. All other collections were begun after the feed had been passed over the catalyst for the times specified. Analysis of the radicals was accomplished by lowering the sapphire rod, under vacuum at 13.5 K, into a TE_{102} microwave cavity and recording the EPR spectrum with a Varian Model V4500 spectrometer. During sequential sampling using the same catalyst the rod was always warmed to a minimum of 160 K, between collections, in order to destroy the matrix.

The g values are reported relative to a phosphorus-doped silicon standard with $g = 1.9987$. Spin concentrations were obtained by double integration of the recorded EPR spectrum of the unknown and the standard. Errors for the spin concentration are estimated to be $\pm 25\%$. For the pure methyl radical spectrum, the spin concentration was calculated by the double-integration method and subsequent spectra of the radical were then compared to this standard spectrum by comparison of peak-to-peak heights. This type of calculation was possible because the shape of the spectra in each case was identical. Although the absolute spin concentration may have an error of $\pm 25\%$, we estimate that a determination of spin concentration ratios for this radical results in an error of $\pm 5\%$ due to elimination of error in the double-integration step and error due to the standard. This type of comparison was not possible for the mixed methyl–methyl peroxy radical spectra because the spectrum shape changed, depending on the percentage of methyl radicals that reacted with the gas-phase molecular oxygen to form methyl peroxy radicals.

EPR analysis of the used solid MgO samples were obtained on a Varian E-6S EPR spectrometer. The g values are reported relative to a phosphorus-doped silicon standard with $g = 1.9987$ and the intrinsic Cr^{3+} line impurity in MgO with $g = 1.9797$. Samples were placed in a quartz EPR tube (3-mm i.d.), evacuated, and cooled for 20 min at 77 K before analysis. All spectra were recorded at 77 K. No special handling procedures were employed in transferring the sample from the reactor to the EPR tube (i.e., the sample was exposed to atmosphere). The samples were evacuated and treated with various gases on a conventional glass vacuum system with an ultimate vacuum of 10^{-6} torr.

As a variation of this procedure, samples were placed in a quartz crucible and heated at the desired temperatures in static air. When the thermal treatment was completed, the samples were then rapidly quenched in liquid nitrogen. The quenched samples were then transferred to a standard EPR tube, again cooled to 77 K, evacuated, and analyzed by EPR.

Surface areas were determined by a gravimetric BET method. Lithium concentrations were determined by atomic absorption on a Varian A-6 spectrometer. X-ray data was obtained on a computer-controlled Siefert-Scintag Pad II automated powder diffractometer.

The gases exiting from the catalysts were analyzed for stable products using an Antek Model 464 LP gas chromatograph. The products were trapped at 77 K for 20 min in a previously evacuated flask and then slowly warmed to ambient temperature before analysis. A Porapak Q column at room temperature was used for the separation of ethane and ethylene, and a Carbowax 600 column at 50 °C was used for the analysis of methanol, formaldehyde, and acetaldehyde.

Table I. Effect of Conditioning on Initial Activity^a

temp, °C [time, h]	radical amt, nmol		
	O_2 , 300 $\text{cm}^3 \text{min}^{-1}$ ^c	vacuum ^e	recondnd (O ₂)
450 [2.5]	3.5 (2.1) ^d	0	3.5
100 [2.0]/450 [2.0] ^b	5.7	0	
100 [2.0]/300 [2.0] ^b	1.3	0	3.0

^a All reactions were carried out under the following conditions: catalyst, MgO(B), $T = 500$ °C, collection period = 25 min (after 2 min on stream), 0.50 g of catalyst, argon flow = $3.8 \text{ cm}^3 \text{ min}^{-1}$, CH_4 flow = $1.14 \text{ cm}^3 \text{ min}^{-1}$, N_2O flow = $0.023 \text{ cm}^3 \text{ min}^{-1}$. ^b Temperature was slowly raised to the second temperature over a period of 30 min. ^c After oxygen treatment the sample was evacuated for a total of 45 min at elevated temperatures. ^d Reaction carried out in the absence of O_2 or N_2O . ^e Catalysts were prepared by decomposition of $\text{Mg}(\text{OH})_2$ under vacuum, without exposure to O_2 at 450 °C.

Table II. Initial Activity over Pure and Doped MgO Samples^a

catalyst	activity, nmol	surf area, m^2/g
MgO(F,LSA) ^b	0.78	59.1
MgO(F,HSA)	2.1	191.6
MgO(B)	3.5	37.5
4.6 wt % Li/MgO(F)	5.4	
4.8 wt % Li/MgO(B)	12.3	14.9
4.8 wt % Na/MgO(B)	2.9	

^a All reactions were run under the following conditions: Preconditioned at 450 °C, 2.5 h, 300 $\text{cm}^3 \text{ min}^{-1}$ O_2 . Reaction at 500 °C, 0.50 g of catalyst, collection period = 25 min (after 2 min on line), argon flow = $3.8 \text{ cm}^3 \text{ min}^{-1}$, CH_4 flow = $1.14 \text{ cm}^3 \text{ min}^{-1}$, N_2O flow = $0.023 \text{ cm}^3 \text{ min}^{-1}$. ^b The MgO was not converted to $\text{Mg}(\text{OH})_2$ before use.

Results

Matrix-Isolated Radicals. The primary radical product from the reactions of methane with O_2 or N_2O over MgO was the methyl radical, but due to secondary reactions with gas-phase molecular oxygen three different EPR signals were observed. The EPR spectra are depicted in Figure 1. Signal a is the pure methyl radical ($\text{CH}_3\cdot$) spectrum, which was obtained when N_2O was the oxidant or at very low O_2 partial pressures. Signal b is the pure methyl peroxy radical ($\text{CH}_3\text{O}_2\cdot$) spectrum. This spectrum was observed only when the ratio of oxygen to radicals was large. Signal c is a mixture of the spectra for methyl and methyl peroxy radicals. This spectrum was observed, to some degree, in all reactions when O_2 was present above background pressures.

The method used to pretreat the MgO had a significant effect on the initial activity. Initial activity is defined here as the amount of methyl radicals collected over a 25-min period commencing after 2 min on stream. Table I summarizes the effect pretreatment has on initial activity. These results were obtained for the reaction of CH_4 with N_2O over MgO(B); however, the same behavior was observed with O_2 in the feed or when doped-MgO samples were used. When MgO was pretreated with O_2 at elevated temperatures, radicals were always produced, but the amount varied depending on the pretreatment temperature and the amount of time the sample was held at the elevated temperatures.

Pretreatment under vacuum at increased temperature resulted in absolutely no radical production. After reaction, these inactive samples appeared to be slightly coked, as indicated by a darkened appearance. By simply reconditioning these samples in O_2 at 450 °C the high activity could be attained. After these reactions the typical white color of the MgO had returned. The used active samples could also be reconditioned and rerun to give activity identical with that in the first run. Although these results indicate that O_2 pretreatment is a necessary requirement for radical formation, later results will show that radicals could be produced, in certain instances, without this pretreatment.

The initial activity also was influenced by the surface area, sample purity, and, in certain cases, cation doping. The initial activity of the different MgO samples examined, along with their specific surface areas, is presented in Table II. The activity of samples of identical purity varied as expected with changing surface area. Comparison of the low- and high-surface-area

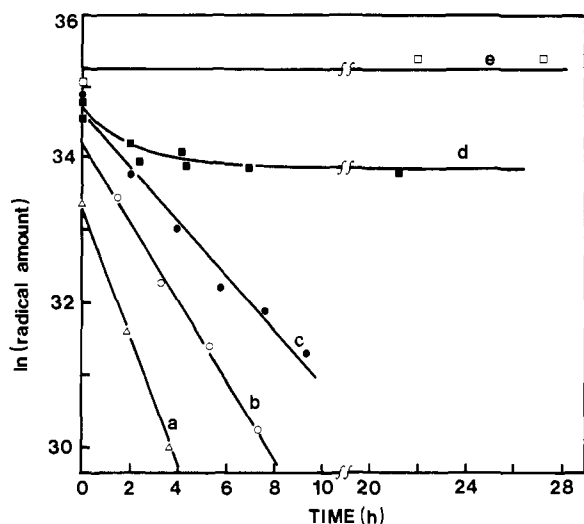


Figure 2. The amount of radicals formed as a function of time on stream. Concentrations are given in \ln of the total number of spins. Except for the flows, all reactions were carried out under the following conditions: catalyst, MgO(B), $T = 500^\circ\text{C}$, collection period, 25 min, 0.50 g of catalyst. Preconditioned at 450°C , 2.5 h, $300\text{ cm}^3\text{ min}^{-1}\text{ O}_2$. Flows: In all reactions CH_4 flow $1.14\text{ cm}^3\text{ min}^{-1}$; (a) Ar 0, N_2O $3.8\text{ cm}^3\text{ min}^{-1}$; (b) Ar $3.8\text{ cm}^3\text{ min}^{-1}$, N_2O $0.023\text{ cm}^3\text{ min}^{-1}$; (c) Ar $3.8\text{ cm}^3\text{ min}^{-1}$, N_2O $0.3\text{ cm}^3\text{ min}^{-1}$; (d) Ar $3.8\text{ cm}^3\text{ min}^{-1}$, O_2 $0.30\text{ cm}^3\text{ min}^{-1}$; (e) Ar $3.8\text{ cm}^3\text{ min}^{-1}$, O_2 $0.023\text{ cm}^3\text{ min}^{-1}$.

MgO(F) samples shows that, as surface area increased, activity for methyl radical formation increased proportionally. Although this behavior was observed for these samples, the remaining results indicate that when the samples of different purity were examined, the activity was influenced to a much greater extent by the sample purity than by variations in the surface area. Activity was found to increase by a factor of 1.7 in going from the undoped MgO(F) sample to the ultrapure undoped MgO(B) sample; however, accompanying this increase there was a decrease in surface area by a factor of 5.1. Lithium doping was found to have a beneficial effect in both MgO samples. Activity increased by a factor of 2.6 and 3.5 for the MgO(F) and MgO(B) samples, respectively. The increase in activity for the Li-doped MgO(B) sample also was accompanied by a decrease in surface area by a factor of 2.5. The surface area decrease was not unexpected as it is well-known that many oxides sinter when doped with alkali metals.^{11,12} Sodium doping was found to have virtually no effect on the initial activity. Doping with iron was also examined and this resulted in no activity increase. These results were obtained from the reactions of CH_4 with N_2O ; however, the same trends existed when the reaction was carried out in the presence of O_2 .

Up to this point, only the initial activity of the samples has been considered. As pointed out earlier, when the used samples were reconditioned the high initial activity was again attained. The fact that the samples could be regenerated suggested that, with the proper conditions, the reactions may be catalytic. Figure 2 gives the results of the long-term catalytic studies. In all cases, preconditioning was with O_2 at elevated temperatures. Lines a, b, and c depict the decrease in activity during the reaction of CH_4 with N_2O over MgO at high, low, and moderate N_2O flow, respectively. The activity declined according to first-order kinetics, and in the best case the half-life was 1.9 h. Plots d and e illustrate how the activity is affected during the reaction of CH_4 with O_2 over MgO at moderate and low flow, respectively. These reactions were obviously catalytic and a steady state was reached. In the case of moderate O_2 flow the reaction was monitored for a period of 9 days, and even after this time the activity had decreased only slightly. The apparent activation energy for this reaction was

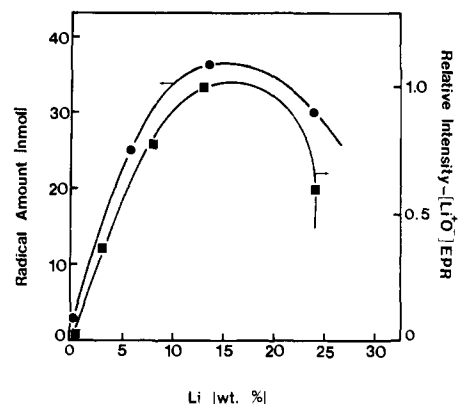


Figure 3. The amount of radicals and $[\text{Li}^+\text{O}^-]$ centers formed as a function of lithium doping into MgO(A). All reactions were carried out under the following conditions: $T = 500^\circ\text{C}$, collection period, 25 min (after 4 h on line), 0.50 g of catalyst, argon flow $3.8\text{ cm}^3\text{ min}^{-1}$, CH_4 flow $1.14\text{ cm}^3\text{ min}^{-1}$, O_2 flow $0.023\text{ cm}^3\text{ min}^{-1}$. Preconditioned at 450°C , 2.5 h, $300\text{ cm}^3\text{ min}^{-1}\text{ O}_2$. The samples were quenched in liquid nitrogen after a 2-h exposure to air at 700°C .

determined, over the temperature range of 500 to 550°C , to be $42 \pm 6\text{ kcal mol}^{-1}$.

Since reaction with O_2 is catalytic, it would seem reasonable that after an extended period of time on line, with O_2 in the feed, the activity of a vacuum-treated catalyst should rise to the steady-state value. A sample of 7.0 wt % Li/MgO(B) was conditioned at 100°C (2 h)/ 450°C (2 h) under vacuum and tested. Although the initial activity was essentially zero, the activity continually increased up to 83.0% of the steady-state value after only 4 h on stream.

When lithium was doped into MgO the initial activity was greatly increased. The amount of lithium doped into the MgO(A) also affected the activity as shown in Figure 3. The points were obtained after 4 h on stream in order to ensure that steady state had been reached. From the plot, it can be seen that activity increased with lithium doping up to a maximum at 13.5 wt % (47.6 mol %). Sintering once again occurred with the surface area falling from $210\text{ m}^2/\text{g}$ in the undoped sample to $54.3\text{ m}^2/\text{g}$ in the sample that contained 13.5 wt % Li. A sample of MgO(A) was doped with sodium to a mole ratio of 50.2%. An increase in CH_3 formation from 2.62 to 6.81 nmol was observed, which is still significantly less than that observed for any of the lithium-doped samples. This sample also sintered with the surface area falling to $19.3\text{ m}^2/\text{g}$.

X-ray powder diffraction of the used, lithium-doped samples, recorded at ambient temperature, indicated two phases were present, MgO and Li_2CO_3 . To ensure that the carbonate alone was not responsible for the reactivity, a sample of Li_2CO_3 was tested and found to have no activity for methyl radical formation. In addition a 7.0 wt % Li/silica (Davison Grade 57) sample was prepared by impregnating silica gel with Li_2CO_3 . Although the activity of this material increased by a factor of 18 from pure silica gel, it was a factor of 12 less than a 7.0 wt % Li/MgO(B) sample and only 33% of the activity exhibited by the pure MgO(B) sample.

Although it was possible to form methyl radicals from methane over pure and doped MgO, the amounts produced were small. Even for the 13.5 wt. % Li/MgO(A) sample, which was found to be the most active catalyst, the amount of radicals produced, assuming a 50% collection efficiency, was only 0.006% of the total methane fed over the catalyst.

Defect Structure of the MgO. Recent work has shown that it is possible to produce a $[\text{Li}^+\text{O}^-]$ center in single crystals of lithium-doped MgO by heating the samples to temperatures of 1000 to 1300°C in the presence of O_2 and then rapidly quenching to 77 K .¹³⁻¹⁶ These paramagnetic centers are characterized by g_\perp

(11) Anderson, P. J.; Livey, D. T. *Powder Metall.* **1961**, *7*, 189.

(12) Mougey, C.; Francois-Rossetti, J.; Imelik, B. "The Structure and Properties of Porous Materials"; Academic Press: New York, 1958; pp 266-292.

(13) Abraham, M. M.; Chen, Y.; Boatner, L. A.; Reynolds, R. W. *Phys. Rev. Lett.* **1976**, *37*, 849.

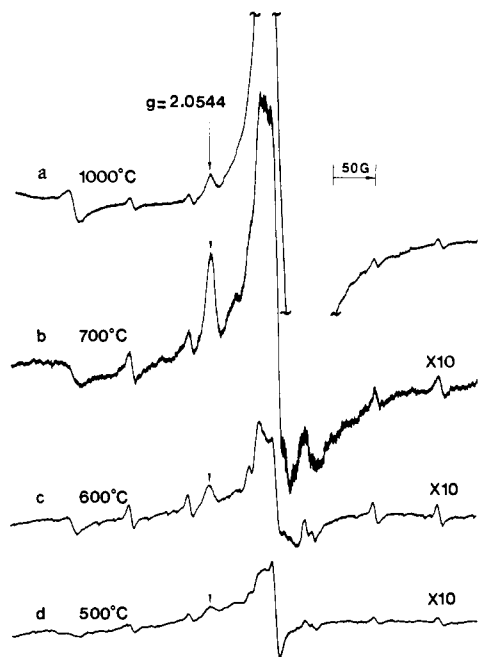


Figure 4. EPR spectra of the $[\text{Li}^+\text{O}^-]$ center in 13.0 wt % Li/MgO(A). Samples were heated in air at the temperature indicated for (a) 10 min and (b)–(d) 2 h. They were subsequently quenched in liquid nitrogen.

$= 2.0545$ and $g_{\parallel} = 2.0049$. In this study, when a 13 wt % Li/MgO(A) sample was heated in air to $T \geq 500$ °C and then quenched in liquid nitrogen, the $[\text{Li}^+\text{O}^-]$ signal was observed. The results of the quenching study are presented in Figure 4. The signal at $g = 2.0544$ is in excellent agreement with the published value of $g_{\perp} = 2.0545$. The $g_{\parallel} = 2.004$ component was not observed due to overlap with the strong Fe^{3+} impurity signal.

The signal intensity was strongly influenced by the conditioning temperature. At temperatures of 1000 and 700 °C, strong signals were observed while the intensity of those produced at 600 and 500 °C was significantly less. The stability of the $[\text{Li}^+\text{O}^-]$ center also was dependent on the conditioning temperature chosen. The centers produced on quenching from 1000 and 700 °C were found to be indefinitely stable on standing at ambient temperatures under a static vacuum or in the presence of air. The center produced on quenching from 600 °C was moderately stable; whereas, the center produced at 500 °C was destroyed within 30 min if the sample was allowed to stand under static vacuum or air at ambient temperature. These centers could be regenerated by simply repeating the thermal treatment.

The intensity of the $[\text{Li}^+\text{O}^-]$ signal varied with respect to the Li content in a manner remarkably similar to that found for the production of $\text{CH}_3\cdot$ radicals, as depicted in Figure 3. The major difference being that no $[\text{Li}^+\text{O}^-]$ signal was detected, as expected, in the absence of any added lithium; whereas, the pure MgO exhibited a small amount of intrinsic activity for $\text{CH}_3\cdot$ radical formation.

Another new signal was observed in the oxygen-pretreated samples and in the used active samples of MgO(B) and Li/MgO(B) that had been cooled slowly from 500 to 25 °C. It must be mentioned that this signal was only observed in the low-surface-area Baker samples and never in the Fisher or Aldrich samples. The EPR spectrum of the new signal is given in Figure 5. A line was observed at $g_{\perp} = 2.045$, which is in good agreement with the value of $g_{\perp} = 2.042$ for O^- on MgO, produced by reacting trapped electrons with N_2O .¹⁷ The corresponding parallel component at $g_{\parallel} \approx 2.001$ was not observed, presumably because it



Figure 5. EPR spectrum of used, active MgO(B). The analysis was obtained with the MgO under vacuum at 77 K.

Table III. Effect of Oxidant Gases in the Product Distribution during the Partial Oxidation of Methane over MgO^a

oxidant flow rate, $\text{cm}^3 \text{min}^{-1}$		stable products, nmol		
N_2O	O_2	ethane	ethylene	methanol
0.00	$\approx 10^{-5}^b$	36.8	3.5	6.9
0.00	0.066	141.0	20.2	16.6 ^c
0.096	$\approx 10^{-5}^b$	186.0	39.2	45.4

^aAll of the above reactions were carried out under the following conditions: $T = 550$ °C, collection period = 30 min, argon and methane flow rates of 5.04 and 1.14 $\text{cm}^3 \text{min}^{-1}$, respectively. The pressure in the catalytic volume was 1.0 torr and about 1.3 g of MgO(F) catalyst was used. ^bAmount of molecular oxygen in the background, after 30 min of pumping, which corresponds to the indicated flow rate. ^cTraces of formic acid and acetaldehyde were also found.

is masked by the strong Fe^{3+} signal. The remaining lines in the spectrum are all due to Cr^{3+} and Mn^{2+} impurities in the MgO lattice. The formation of O^- on MgO by thermal treatment has been speculated, but the signal has previously remained undetected by EPR.¹⁸ Martens et al.¹⁹ postulated its formation due to hydrogen and oxygen release during the thermal decomposition of $\text{Mg}(\text{OH})_2$ to form the oxide. This is the first report of the EPR signal of O^- or a V-type center being formed in MgO by means other than irradiation or thermal quenching.

The signal described here was very stable. It was not destroyed upon allowing the sample to stand in air at ambient temperature for 2 months or by heating the sample to 450 °C under vacuum for 10 h. Moreover, the signal could not be eliminated by reaction with gas-phase molecules including CO , CH_4 , or O_2 , and the signal was not altered when the sample was in the presence of 175 torr of gas-phase O_2 . These results confirm that the new species is not on the surface of the MgO. The signal also was not destroyed by UV irradiation; however, a new signal at $g_{\perp} = 2.035$ was observed. This line is due to the V_1 center which has been previously reported.²⁰ The corresponding component at $g_{\parallel} = 2.0032$ also was not observed due to the strong Fe^{3+} signal.

The possible role of O_2^- in forming methyl radicals was explored. In earlier work it was demonstrated that O_2^- could be produced on MgO at low temperatures by preadsorbing hydrogen²¹ or other hydrocarbons^{22,23} prior to O_2 exposure. The MgO preconditioning in these studies was much more severe than any conditioning used here; however, an attempt was made to produce O_2^- by preadsorption of CH_4 . A sample of previously conditioned MgO(B) was evacuated, exposed to 300 torr of methane at ambient temperature for 25 min, evacuated, exposed to 150 torr of O_2 at ambient temperature for 20 min, evacuated, and cooled to 77 K for 20 min before the EPR analysis. No O_2^- signal was observed;

(14) Chen, Y.; Tohver, H. T.; Narayan, J.; Abraham, M. M. *Phys. Rev. B* **1977**, *16*, 5535.

(15) Boldu, J. B.; Abraham, M. M.; Chen, Y. *Phys. Rev. B* **1979**, *19*, 4421.

(16) Abraham, M. M.; Unruh, W. P.; Chen, Y. *Phys. Rev. B* **1974**, *10*, 3540.

(17) Wong, N.-B.; Lunsford, J. H. *J. Chem. Phys.* **1971**, *55*, 3007.

(18) Che, M.; Tench, A. J. *Adv. Catal.* **1982**, *31*, 77.

(19) Martens, R.; Geutsh, H.; Freund, F. *J. Catal.* **1976**, *44*, 366.

(20) Lunsford, J. H. *J. Phys. Chem.* **1964**, *68*, 2312.

(21) Ito, T.; Yoshioka, M.; Tokuda, T. *J. Chem. Soc., Faraday Trans. 1* **1983**, *79*, 2277.

(22) Morris, R. M.; Klabunde, K. J. *Inorg. Chem.* **1983**, *22*, 682.

(23) Garrone, E.; Zecchina, A.; Stone, F. S. *J. Catal.* **1980**, *62*, 396.

thus it seems unlikely that this species could be responsible for the formation of methyl radicals.

Stable Product Formation. A preliminary study was carried out to determine the distribution and concentration of stable products formed during the reaction of methane with O_2 and N_2O over $MgO(F)$. The results of this study are summarized in Table III. The dominant product was ethane, which probably results from the coupling of methyl radicals. Oxygen was much less selective than nitrous oxide. With N_2O as the oxidant a modest amount of methanol was also formed.

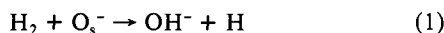
Discussion

Results from the initial activity studies and the long-term runs provide conclusive evidence that O_2 is required both to generate and to maintain a steady-state concentration of active sites. It is unlikely, however, that O_2 itself or that a related ion such as O_2^- is responsible for hydrogen atom abstraction. The standard pretreatment involved heating the oxidized catalyst under vacuum to 500 °C, which required approximately 40 min. Such pretreatment undoubtedly would have removed adsorbed O_2 and would have destroyed any O_2^- species that may have been present.⁷ Nevertheless, as shown in Table I, such catalysts were initially active for $CH_3\cdot$ formation even in the absence of oxidant.

We propose that methyl radicals are formed at O^- ions on the surface of pure and lithium-doped MgO . There is both theoretical and experimental evidence to support the presence of such ions in MgO and the reactivity of these ions with hydrogen. The theoretical evidence will be considered first.

Kunz and co-workers²⁴ initially showed that on a micro [111] face of a MgO crystal a $(Mg^+O^-)_3$ cluster is 3.7 eV more stable than a $(Mg^{2+}O^{2-})_3$ cluster. In addition, at a nickel ion vacancy on the surface of NiO , the O_3^- cluster is more favorable in the 40^2-10^- configuration than with five O^{2-} ions.²⁵ On both the MgO surface and at the Ni defect site a stable bond is formed between O^- and H.

More recently this theoretical work has been extended by Colbourn et al.^{26,27} who examined the energetics of hydrogen adsorption at defect sites on both pure and doped MgO . This group concluded that the dissociative chemisorption of H_2 on MgO requires the presence of defects and that, at anion vacancies, V^- centers and O_s^- ions the overall process is exothermic. Most notable is the result that on the planar [001] surface the reaction



is exothermic to the extent of 20 kcal/mol. Moreover, there is a marked increase in the OH^- bond strength as nearest neighbor coordination is reduced. For comparison purposes, one should keep in mind that the C-H bond strength in CH_4 and the H-H bond strength in H_2 are nearly identical at approximately 104 kcal mol^{-1} .²⁸

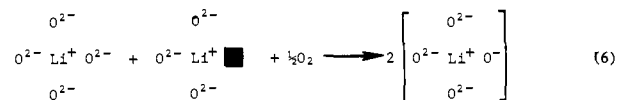
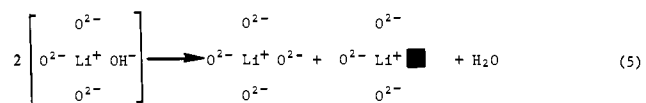
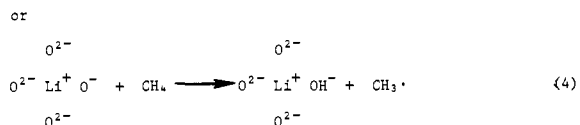
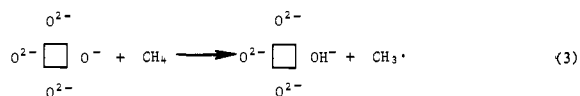
From an experimental standpoint there is considerable evidence that O_s^- formed by the reaction



is very effective in abstracting hydrogen from simple alkanes, including methane.⁵ In the present experiments it is unlikely that reaction 2 would have been responsible for the O_s^- ions since (a) the electrons would not have been available on an oxidized surface of MgO and (b) N_2O was found to be a relatively ineffective oxidant in this case.

It seems more reasonable that the O_s^- ions were formed thermally at defect and lithium impurity sites. The EPR results depicted in Figure 4 provided evidence that the $[Li^+O^-]$ centers were present in the lithium-doped MgO samples of this study, even at temperatures as low as 500 °C. Moreover, a good correlation was found between the rate of methyl radical formation and the

Scheme I



concentration of $[Li^+O^-]$ centers as the lithium content was varied (Figure 3). Although the analogous V-type centers were not detected on all of the undoped MgO samples, it is possible that they existed at the elevated temperatures, but on cooling their concentration fell below detection limits.

The work of the Oak Ridge group provides insight into the formation of O^- centers in lithium-doped MgO crystals.¹³⁻¹⁶ In this material the $[Li^+O^-]$ centers are believed to originate from lithium oxide precipitates which at high temperatures give rise to "microgalaxies" containing large concentrations of substitutional lithium ions. X-ray powder diffraction of our samples has shown the presence of an analogous lithium carbonate precipitate which should also be capable of forming the Li^+ -rich microgalaxy.

The fact that sodium was less effective in generating active sites than lithium also suggests the importance of a substitutional defect site. The ionic radius of Mg^{2+} is 0.66 Å and that of Li^+ is 0.68 Å, whereas the radius of Na^+ is 0.97 Å.²⁸ Sodium likewise is less effective in producing stable $[Na^+O^-]$ centers in MgO single crystals.¹⁴

The previous results suggest that there are actually two O_s^- sites responsible for methyl radical formation. Over pure MgO , O^- ions associated with intrinsic cation vacancies are responsible for methyl radical formation. In addition to these sites, $[Li^+O^-]$ centers are formed on the lithium-doped samples, and these are responsible for the increased activity in the doped samples. The catalytic cycle in Scheme I may be written to describe the results.

Here, O_2 is used to replace the surface oxygen, which is removed as water. It is important to note that oxygen was required both in the steady-state formation of methyl radicals and in the formation of $[Li^+O^-]$ sites. Unlike the case with transition-metal oxides, no variation in oxidation state of the metal ion is required. The rather large activation energy of 42 kcal mol^{-1} probably involves either the mobility of species across the surface, e.g., reaction 5, or the formation of O_s^- via an endothermic reaction.

The distribution of stable products (Table III) indicates that the primary reaction is the coupling of methyl radicals to form ethane. Moreover, the amount of ethane formed was of the same order of magnitude as the amount of $CH_3\cdot$ radicals that would have been collected under similar conditions. Thus, as in the case of gas-phase allyl radical coupling to form the stable product 1,5-hexadiene,⁹ it appears that the coupling of gas-phase methyl radicals was also responsible for the formation of ethane. The methanol probably is formed via a mechanism involving surface methoxide ions, which are then converted to methanol upon reacting with water in the system. This mechanism is analogous to that proposed in the partial oxidation of CH_4 over a Mo/SiO_2 catalyst.¹ The major difference being that over MgO the O^- was derived from O_2 ; whereas, with Mo/SiO_2 the O^- was derived from N_2O . The activation of methane for partial oxidation over MgO

(24) Kunz, A. B.; Guse, M. P. *Chem. Phys. Lett.* **1977**, *45*, 18.

(25) Surratt, G. T.; Kunz, A. B. *Phys. Rev. Lett.* **1978**, *40*, 347.

(26) Colbourn, E. A.; Kendrick, J.; Mackrodt, W. C. *Surf. Sci.* **1983**, *126*, 550.

(27) Colbourn, E. A.; Mackrodt, W. C. *Surf. Sci.* **1982**, *117*, 571.

(28) Weast, R. C., Ed. "CRC Handbook of Chemistry and Physics", 62nd ed.; CRC Press: Boca Raton, FL, 1982; pp F-183, F-191, F-175.

is currently being investigated under more conventional catalytic conditions.

Conclusions

Gas-phase methyl radicals may be produced in a catalytic manner from CH₄ over pure and lithium-doped MgO. The results suggest that surface O⁻ ions are responsible for hydrogen atom abstraction, and in the lithium-doped samples the O⁻ is present as a [Li⁺O⁻] center. This center is formed from the interaction of substitutional Li⁺ ions with molecular oxygen at high tem-

peratures. Ethane probably occurs via the coupling of the gas-phase methyl radicals, but the conversion of methane is quite small.

Acknowledgment. We thank David L. Myers and Han-Fan Liu for their experimental assistance. We also acknowledge the conceptual contributions of Dr. John Kolts. The work was supported by the Division of Basic Energy Science, Department of Energy.

Registry No. MgO, 1309-48-4; methane, 74-82-8; methyl radical, 2229-07-4; lithium, 7439-93-2; hydrogen, 1333-74-0.

Cation Transport from Multiple Alkali Cation Mixtures Using a Liquid Membrane System Containing a Series of Calixarene Carriers

Steven R. Izatt,[†] Richard T. Hawkins, James J. Christensen,* and Reed M. Izatt*

Contribution from the Departments of Chemistry and Chemical Engineering, and Contribution No. 348 from the Thermochemical Institute, Brigham Young University, Provo, Utah 84602.

Received March 21, 1984

Abstract: Several new *p*-tert-pentylcalixarenes have been synthesized. These and other calixarenes have been used to study carrier-mediated alkali-metal cation fluxes at 25 °C in H₂O-(organic solvent)-H₂O liquid membranes. In addition to single cation systems, all possible equimolar, two-, three-, and four-cation mixtures of NaOH, KOH, RbOH, and CsOH were used in the study. In each case, alkali cation transport was coupled with the reverse flux of protons. Selective transport of Cs⁺ over Rb⁺, K⁺, and Na⁺ was seen in all mixtures studied. The greatest selectivity for Cs⁺ was found for calix[4]arenes, but the largest flux of Cs⁺ as well as the other alkali cations was seen with the calix[6]arenes and calix[8]arenes. The greater flux in these latter cases may be a result of each calixarene binding two cations. In experiments at low [Cs⁺]-to-[Rb⁺] ratios, *p*-tert-butylcalix[6]arene transports Rb⁺ over Cs⁺. As these ratios increase, transport of Cs⁺ becomes favored over that of Rb⁺, indicating that the cation flux depends, in part, on the relative concentrations of the cations in the source phase.

Calixarenes¹ are macrocyclic phenol-formaldehyde condensation products similar in structure to certain cyclic polyethers which are noted for their size-related selectivity in binding cations.² Calixarenes have been suggested as potential enzyme mimics because they possess a toruslike architecture similar to that of cyclodextrins.³ The appealing features of cyclodextrins (which are naturally occurring macrocyclic glucose polymers containing a minimum of 6-D(+)-glucopyranose units, attached by α-(1,4) linkages) are their abilities to form host-guest complexes by trapping organic compounds, small ions, and gases in their toruslike cavities and to mimic enzyme functions.⁴

The calixarenes were first reported by Zinke and Ziegler in 1944.⁵ More recently, Gutsche and his co-workers have demonstrated the condensation of *p*-tert-butylphenol and formaldehyde to yield *p*-tert-butylcalix[4]arene, -calix[6]arene, and -calix[8]arene^{1,3,6} (Figure 1). Kämmerer and Happel have published methods for the multistep synthesis of several calixarenes, including a calix[5]arene and a calix[7]arene.⁷

Several unique features of calixarenes have been noted. First, their synthesis, in at least one case, is promoted by a template effect, e.g., the interaction between *p*-tert-butylcalix[6]arene and Rb⁺.⁶ Second, they form molecular complexes with small molecules in the solid state.⁸ Third, they are weak Brønsted-Lowry acids and act as anionic carriers in liquid membrane transport of alkali cations.⁹ In a recent investigation,⁹ we found that *p*-tert-butylcalix[4]arene, -calix[6]arene, and -calix[8]arene are effective in transporting individual alkali-metal cations from the aqueous solutions across haloform liquid membranes. Specifically,

these calixarenes transported Cs⁺ at a much higher rate than they did other alkali cations when the source phase was a solution of the metal hydroxide. Selectivity for Cs⁺ increased in the order [8] < [6] < [4] although the Cs⁺ flux increased in the reverse order.

In the present study, the synthesis of several new calixarenes is reported. In addition, calixarene-mediated cation fluxes have been determined for Na⁺, K⁺, Rb⁺, and Cs⁺ (anion: OH⁻) both in single-cation systems and in all possible two-, three-, and four-cation mixtures of these cations using a H₂O-CCl₄-CH₂-Cl₂-H₂O liquid membrane system. The purpose of the transport investigation was to learn whether the selectivity for Cs⁺ observed earlier⁹ is maintained in the mixtures and to determine the effect

(1) (a) Gutsche, C. D.; Muthukrishnan, R. *J. Org. Chem.* **1978**, *43*, 4905-4906. (b) Gutsche, C. D.; Levine, J. A. *J. Am. Chem. Soc.* **1982**, *104*, 2652-2653. (c) Ninagawa, A.; Matsuda, H. *Makromol. Chem. Rapid Commun.* **1982**, *3*, 65-67.

(2) (a) Lab, J. D.; Izatt, R. M.; Christensen, J. J.; Eatough, D. J. In "Coordination Chemistry of Macrocyclic Compounds"; Melson, G. A., Ed.; Plenum Press: New York, 1979; pp 145-217. (b) Lamb, J. D.; Izatt, R. M.; Swain, C. S.; Christensen, J. J. *J. Am. Chem. Soc.* **1980**, *102*, 475-479.

(3) Gutsche, C. D. *Acc. Chem. Res.* **1983**, *16*, 161-170.

(4) (a) Fendler, J. H. "Membrane Mimetic Chemistry"; Wiley: New York, 1982. (b) Bender, M. L.; Komiya, M. "Cyclodextrin Chemistry"; Springer-Verlag: Berlin, 1978. (c) Saenger, W. *Angew. Chem., Int. Ed. Engl.* **1980**, *19*, 344-362. (d) Tabushi, I. *Acc. Chem. Res.* **1982**, *15*, 66-72.

(5) Zinke, A.; Ziegler, E. *Chem. Ber.* **1944**, *77*, 264-272.

(6) Gutsche, C. D.; Dhawan, B.; No, K. H.; Muthukrishnan, R. *J. Am. Chem. Soc.* **1981**, *103*, 3782-3792.

(7) Kämmerer, H.; Happel, G. *Makromol. Chem.* **1980**, *181*, 2049-2062.

(8) Zinke, A.; Kretz, R.; Leggewie, E.; Hössinger, K.; Hoffmann, G.; Weber v. Ostwalden, P.; Wiesenberger, E.; Sobotka, M. *Monatsh. Chem.* **1952**, *83*, 1213-1227.

(9) Izatt, R. M.; Lamb, J. D.; Hawkins, R. T.; Brown, P. R.; Izatt, S. R.; Christensen, J. J. *J. Am. Chem. Soc.* **1983**, *105*, 1782-1785.

[†] Present Address: Homer Research Laboratory, Bethlehem Steel Corp., Bethlehem, PA 18016.